

University of Mississippi

eGrove

Honors Theses

Honors College (Sally McDonnell Barksdale
Honors College)

2009

Dissection of NCAD12: Distinctive Characteristics of Domains 1 and 2

Brittany Nicole Rogers

Follow this and additional works at: https://egrove.olemiss.edu/hon_thesis

Recommended Citation

Rogers, Brittany Nicole, "Dissection of NCAD12: Distinctive Characteristics of Domains 1 and 2" (2009).
Honors Theses. 2110.

https://egrove.olemiss.edu/hon_thesis/2110

This Undergraduate Thesis is brought to you for free and open access by the Honors College (Sally McDonnell Barksdale Honors College) at eGrove. It has been accepted for inclusion in Honors Theses by an authorized administrator of eGrove. For more information, please contact egrove@olemiss.edu.

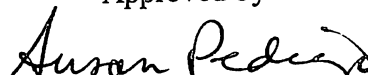
Dissection of NCAD12: Distinctive Characteristics of Domains 1 and 2

By
Brittany Rogers

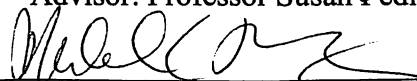
A thesis submitted to the faculty of The University of Mississippi in partial fulfillment of
the requirements of the Sally McDonnell Barksdale Honors College.

Oxford
May 2009

Approved by



Advisor: Professor Susan Pedigo



Reader: Professor Mike Mousing



Reader: Professor Randy Wadkins

ABSTRACT

BRITTANY ROGERS: Dissection of NCAD12: Distinctive Characteristics of Domains 1 and 2

(Under the direction of Dr. Susan Pedigo)

The cadherin superfamily of cell surface adhesion molecules have long been recognized for their crucial roles in morphogenesis, and controlled growth and turnover in adult tissues. Neural cadherins (NCAD) are involved in the cell to cell adhesion of neural tissue. Neural cadherin molecules share a common structure with the members of its superfamily including an amino terminal extracellular region, a transmembrane region and a carboxyl-terminal cytoplasmic region. It contains five folded domains in its extracellular region that are seven strand β -barrel modules of the immunoglobulin type. These modular domains are then connected by a seven amino acid sequence known as linker regions. It has been reported that calcium binding and Domains 1 and 2 are essential to adhesion. Previous studies of Epithelial cadherin (ECAD) have characterized the stability as a function of temperature and denaturant concentration. Here, we report studies of the component modules of dissected NCAD 12: the extracellular domains individually (NCAD 1 and NCAD 2) and the two-Domain construct NCAD 12. Ultra-violet (UV) spectra of all NCAD constructs were used to determine stock concentrations and molar extinctions coefficients. Thermal denaturation was monitored via circular dichroism (CD) in the presence and absence of calcium. Data showed a stable NCAD 1 with an uncharacteristically high melting temperature. NCAD 2 was very similar to ECAD 2 in that the core domain was quite stable and it is destabilized by the adjacent linker segments. Domain 2 constructs were stabilized by calcium. The primary melting transition for the two-Domain construct, NCAD 12, was similar to the melting transition

for NCAD 2, indicating that the stability of the construct is dominated by that of Domain 2. However, NCAD 12 also showed the high temperature melting transition as seen for constructs containing Domain 1. This second transition makes data analysis problematic. Our studies indicate that formation of this “stable” species is reversible and independent of protein and calcium concentration.

TABLE OF CONTENTS

LIST OF TABLES AND FIGURES.....	v
LIST OF ABBREVIATIONS.....	vi
INTRODUCTION.....	1
MATERIALS AND METHODS.....	5
RESULTS.....	10
DISCUSSION.....	18
CONCLUSION.....	24
REFERENCES.....	25

LIST OF TABLES AND FIGURES

Table 1:	Molecular weights of protein constructs as determined by SDS-Page, Mass Spectroscopy and Amino Acid Sequence	10
Table 2:	Extinction Coefficients as determined by Ultraviolet Spectroscopy.....	13
Table 3:	Temperature -Melting compilation.....	14
Figure 1:	Structure and sequence comparison of Neural Cadherin.....	2
Figure 2:	SDS-Page protein Mass Analysis	11
Figure 3:	Spectral Comparison of Neural Cadherin Domains	12
Figure 4:	Calcium-Dependent Temperature Induced Denaturation of NCAD Constructs.....	16
Figure 5:	Reversibility: Unfolding and refolding experiments.....	17

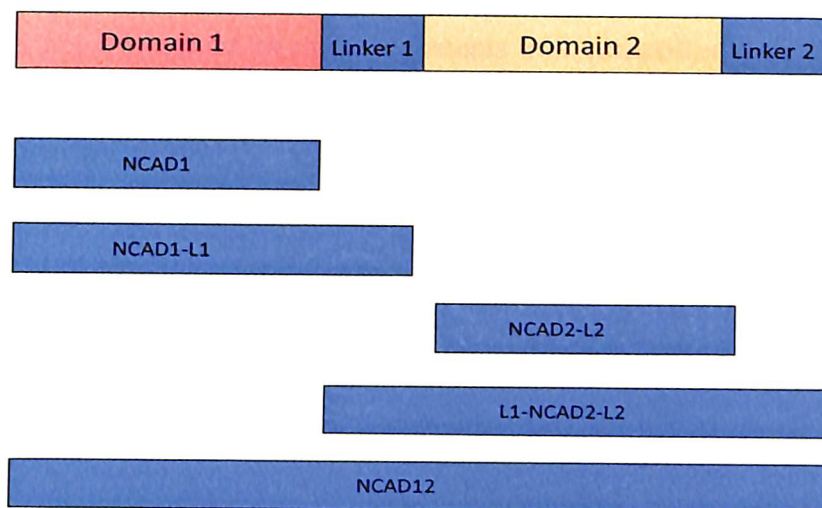
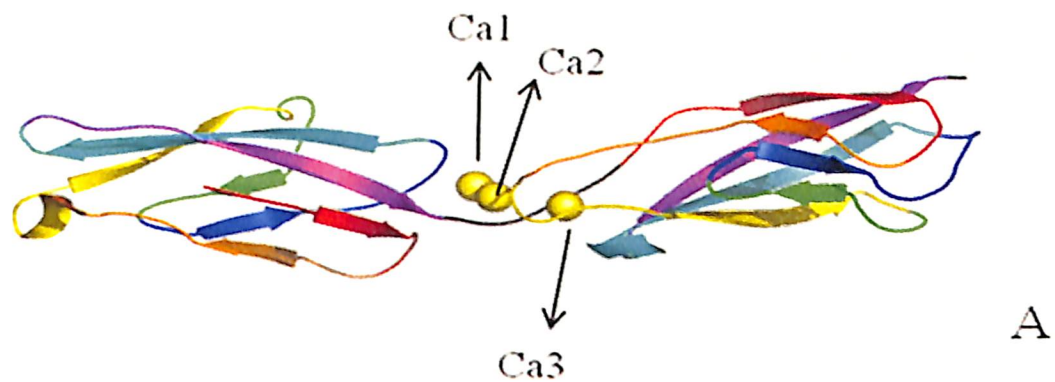
LIST OF ABBREVIATIONS

CD	circular dichroism
EC	extracellular
ECAD	epithelial cadherin
ECAD 2	epithelial cadherin, domain 2
ECAD12	epithelial cadherin, domain 1 + domain 2
HEPES	N-2-Hydroxyethylpiperazine-N'-[2-ethanesulfonic acid]
IPTG	isopropylthiogalactoside
NCAD	neural cadherin
NCAD1	neural cadherin, domain 1
NCAD1-L1	neural cadherin, domain 1 + linker 1
NCAD2	neural cadherin, domain 2
L1-NCAD2-L2	neural cadherin, domain2 + linker 1 + linker 2
NCAD12	neural cadherin, domain 1 + domain 2 + both linkers
SDS PAGE	sodium dodecylsulfate polyacrylamide gel electrophoresis
SEC	size exclusion chromatography
Tris	tris(hydroxymethyl)aminomethane
W2	tryptophan, second residue in NCAD sequence

INTRODUCTION

Cadherins are transmembrane proteins responsible for calcium mediated cell to cell interaction of identical cells. The cadherin superfamily shares a common domain organization. Cadherin structures consist of an amino-terminal extracellular region, a transmembrane region and a carboxyl terminal cytoplasmic region. In the classical cadherin family the extracellular region contains five modular domains that are linked by a seven amino acid peptide (1). These linker regions are important in providing the interface in which calcium binds (Figure 1A). The extracellular domains exhibit homophilic interactions between adjacent cadherin structures in two ways: Lateral-dimerization occurs between cadherins on the same cell surface. Adhesive interactions occur between cadherins from opposing cell surfaces (2, 3). The calcium binding at the interfaces between domains links the modular domains to transduce the signal of adhesion to the cytoskeleton. This causes tension in the cytoskeleton network that promotes the adhesion process by a downstream signaling mechanism. This communication links the actin cytoskeleton of neighboring cells (4-6). Thus, calcium binding causes the extracellular domains become a more stable cooperative structure.

The minimal functional unit that binds calcium and dimerizes contains the first two extracellular domains (Figure 1B). The modular domains are seven-strand β -sheet structures of the classic immunoglobulin type fold (2). These domains fold when they are isolated from the rest of the protein. This facilitates studies of their unique properties.



C. Sequence Comparison

	1	10	20	30	40	50	60
NCAD1-L1	DWVIPPINL--	PENSR-GPFPQELVRI	RIRSDRDKNLS--	LRYSVTGP	GADQPPTGIF	IINPISGQL	
	...	:	:	:
NCAD2-L2	EFLHQVWNGSVPE	EGSKPGTYVMTV	TAIDADDPNAL	NGMLRYRILS	QAPSTPSP	NMFTINNETGDI	
		70	80	90	100		
NCAD1-L1	-SVTKPLDRE	ELIARFHLRAH	AVDINGNQ--	VENPIDIVIN	VIDMNDNRP		
	:
NCAD2-L2	ITVAAGLDREK	VQQYTLIIQAT	DMEGNPTYGL	SNTATAVIT	VDVNDNPP		

Figure 1: Structure and sequence comparison of Neural Cadherin. (A) Ribbon drawing of NCAD 12 made in PyMol (www.pymol.org). β -Sheet regions are indicated as followed: sheet a, red; sheet b, orange; sheet c, yellow; sheet d, green; sheet e, blue; sheet f, cyan; sheet g, magenta; Linker 1 and Linker 2 are black; yellow spheres represent calcium ions. (B) Schematics of NCAD Constructs. Linker 1 residues are 100 thru 106. Linker 2 residues are 213 thru 219. (C) Alignment of primary structure of NCAD 1 and 2 to illustrate similarities and differences in amino acid sequence.

The N-terminal domain (Domain 1) is responsible for mediating protein-protein interactions by undergoing a calcium-dependent conformational change (7). Calcium is essential to the adhesion process. The three calcium ions that bind at the interface between domains are chelated by the linker region and other highly conserved residues in the loops that connect the β -sheets in the EC domains (8, 9). Figure 1C shows an alignment of the primary structure of the first two EC domains of NCAD. The amino acids that bind calcium are shown in bold.

Cadherins are important in morphogenesis and controlled growth in human tissue architecture. There are several different types of cadherins named according to which tissue they predominate: E-Cadherin, found in epithelial tissue, P-Cadherin, found in the placenta, and N-Cadherins, found in neurons. During the development of tissue, ECAD and NCAD are differentially expressed (10). This implies that they confer characteristics required for specific applications. Because of the modular structure of the extracellular domains, our lab has been interested in characterizing their unique properties.

The first two domains of ECAD have been well characterized by studying the modular domains individually (11-13). The work in this thesis reports similar studies of NCAD and summarize data collected over a several year period by undergraduate researchers in the laboratory of Dr. Susan Pedigo. We used fluorescence, UV-vis, and CD spectroscopy to characterize the single domain constructs NCAD 1, NCAD 2, and the two-Domain construct NCAD 12. Further, we looked at the relative stability of the constructs using thermal denaturation, and the reversibility of these unfolding transitions. In general, the studies reported here are similar to those of ECAD. The exception to the

characteristics of ECAD is the anomalously high temperature melting transition of Domain 1 in NCAD.

MATERIALS AND METHODS

Recombinant plasmid construction and cloning:

The cDNA clone of the entire coding sequence for NCAD from mouse was provided by Prof. Shapiro (Columbia University) in an unknown vector with ampicillin resistance. Primers for each of the constructs were designed following the protocol specified in the Xa/LIC cloning kit (Novagen). PCR amplification was conducted with KOD HiFi DNA Polymerase (Novagen) and dNTPs for 25 cycles following the protocol for KOD HiFi DNA Polymerase. The PCR products were purified using a standard Plasmid Prep Kit (Qiagen). The purified PCR products were treated with T4 DNA Polymerase in the presence of dATP to create 5' overhang sequences. The treated PCR products were annealed to the pET-31b Xa/LIC vector at the Xa/LIC cloning site located immediately after the N-terminal tags. Competent XL1-blue cells were transformed and cell stocks were made from a single colony. Plasmid purified from the XL1-blue cells was sequenced and used to transform BL21(DE3) cells. Colonies were screened for expression of proteins of the correct molecular weight (SDS-PAGE).

Overexpression and Purification:

Bacterial cultures were grown in 1 liquid cultures for 2 hours after induction. Protein was recovered from the inclusion body fraction and purified using His Tag chromatography using standard protocols. Immobilized trypsin was used to cleave the N-

terminal affinity label from the constructs. Size Exclusion Chromatography (SEC) was used as the final purification step and for buffer exchange. The working buffer for all experiments was 10 mM HEPES, 140 mM NaCl, pH 7.4 (SEC buffer). Protein stocks were screened for the presence of noncovalent dimer by analytical SEC using a Superose 12 column at 0.5 mL/min with SEC buffer as the mobile phase. Stocks contained a significant fraction of dimer that was found to be quite stable to dilution. In order to reduce the concentration of this dimeric species, stocks were heated to 37 °C for 15 minutes. This simple “heat treatment” reduced the dimer concentration significantly in the stocks.

Mass of the Protein Products:

Mass of protein product was found by using two different methods: SDS-PAGE separation by protein size and mass spectroscopy by charge to mass ratio through electric field. Mass spectroscopy samples were 20 µL at 10 µM protein stock and sent to Stanford University Mass Spectroscopy lab for analysis.

Extinction Coefficient:

Molar absorption of the purified protein was determined by using the UV-vis spectrometer in the native and denatured state of the protein. Denatured state was achieved by diluting 25 µl of protein stock with 105 µl of 8 M GdnHCl. The native state was a solution of 25 µl of protein stock and 105 µl of SEC buffer. The stock protein concentration for the denatured state was calculated using the equation

$$A = \epsilon b C \quad (1)$$

where A was measured with UV- vis and is the absorbance at 280 nm, ϵ is equal to the molar absorption coefficient, b is the path length, and C is the protein concentration. ϵ

used for the protein in the denatured state was calculated based upon the number of Tyrosine and Tryptophan residues in each protein construct. According to Eq. 2

$$\epsilon(280) = (\# \text{ Trp})(5,500) + (\# \text{ Tyr})(1,490) + (\# \text{ Cystine})(125) \quad (2)$$

where $\epsilon(280)$ is in units of $\text{M}^{-1}\text{cm}^{-1}$. The value of concentration of the stock was found and then used to calculate the value of $\epsilon(280)$ in the native state.

Spectral Studies:

Ultraviolet Spectroscopy A UV-scan of purified protein was taken on Cary 50 Bio UV-vis Spectrophotometer in order to determine the stock concentrations and the molar absorption coefficient of all protein constructs using a 4 mm x 1 cm quartz cuvette. Data were taken from 350 to 200 nm and blank corrected. No significant scattering of light was observed indicating that the protein in the stock was soluble.

Circular Dichroism Spectroscopy CD scans were performed on an Aviv Model 202SF CD spectrometer from 200 nm to 300 nm, with an averaging time of 5 sec. These scans were performed in the apo state and in the presence of 5 mM CaCl_2 or 1 M NaCl. The protein concentration for all protein stocks was found to be $\sim 50 \mu\text{M}$ using a 0.2 mm path length. Protein solutions were prepared by mixing 42 μl of protein stock with either 2 μl of SEC buffer (Apo-condition), 2.3 mg NaCl (1 M NaCl condition) or 2 μl of 100 mM CaCl_2 stock (5 mM calcium condition).

Fluorescence Spectroscopy Fluorescence spectra were taken at an excitation of 290 nm from 300 to 400 nm in 2 sec increments. The angles were set at 47.2 °C for both excitation and emission. The spectra were taken in the apo state of 5 μM of protein stock.

and governed by the equilibrium constant K given in Eq. 3 for which $[U]$ is the concentration of the unfolded state and $[N]$ is the concentration of the native state at any point along the unfolding profile.

$$K = \frac{[U]}{[N]} = e^{-\Delta G / RT} \quad (4)$$

The mole fraction of unfolded species in a solution is given by Eq. 5.

$$f_u = \frac{K}{1 + K} \quad (5)$$

The f_u varies between 0 and 1 as the protein is unfolded and must be corrected for the actual span and offset of the experimental data using the equation below in which the span is the difference between the unfolded and native baselines and the offset is the native baseline.

$$\text{Signal} = f_u * \text{span} + \text{offset} \quad (6)$$

Temperature-induced unfolding is governed by the Eq. 7 shown below

$$\Delta G = \Delta H_m^0 \left(1 - \frac{T}{T_m}\right) + \Delta C_p^0 \left(T - T_m - T \ln \frac{T}{T_m}\right) \quad (7)$$

where ΔH_m^0 is the enthalpy of unfolding at the melting temperature, T_m is the melting temperature and ΔC_p^0 is the heat capacity at the melting temperature. Thus, the temperature-induced denaturation experiments were fit to Eqs. 6 and 7. The temperature denaturation data required that the value of ΔC_p^0 be fixed. In these fits, ΔC_p^0 was constrained to values of 0, 0.5 and 1.0 kcal/mol•K.

RESULTS

Size of Constructs

Table 1 shows the results of the mass analysis of the various constructs. The data from mass spectrometric analysis of the constructs is remarkably similar to the predicted value based on the amino acid sequence. The values obtained differ by less than an extra carbon atom. The estimated size of the constructs based on their migration in SDS-PAGE was also quite similar to the expected value. In both single domain cases, the constructs with the linkers was larger than without the linkers, as we would expect.

TABLE 1: Molecular Weights of Protein Constructs

METHOD	NCAD 1	NCAD 1-L1	NCAD2	L1-NCAD 2-L2	NCAD 12
Calculated ^a	11025	11868	11631	13226	24233
Mass Spectroscopy ^b	11025	11867	11756	13162	24229
SDS-Page ^c	10660	11200	10140	12360	23530

^a Based on amino acid sequence as determined using Peptide Properties Calculator (<http://www.basic.northwestern.edu/biotools/proteincalc.html>)

^b Mass analysis at Stanford University Mass Spec Facility

^c Estimated molecular weight of purified construct compared to a Sigma Low Molecular Weight Standard.

Purity

Figure 2 shows an SDS-PAGE gel that shows that all protein samples were free of contaminants except for the NCAD 1-L1 stock which had some contamination from a higher molecular weight species. This species appears to be residual full length recombinant protein that was not cleaved by trypsin during the protein preparation.

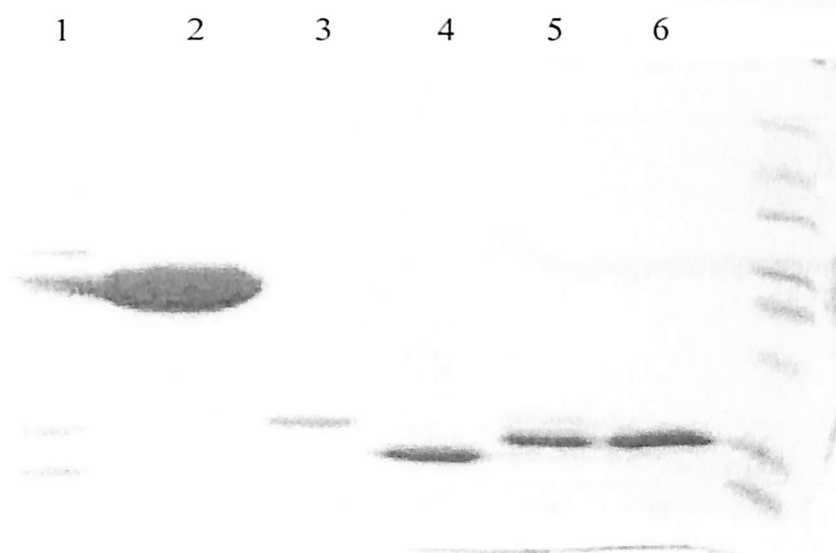


Figure 2: SDS-PAGE gel of the constructs studied. Lane Identities: 1. Standard; 2. NCAD 12; 3. L1-NCAD 2-L2; 4. NCAD 2; 5. NCAD 1-L1; 6. NCAD 1

Spectral Comparison

The UV spectra of each protein construct were typical for tryptophan containing proteins with a local maximum at 280 nm and a shoulder at 290 nm (**Figure 3A**). The shape of the NCAD 1 spectrum at 280 nm showed less signal than that of NCAD 2. The spectra for Domains 1 and 2 were summed and are represented by the solid line. The sum of the spectra from the individual domains NCAD 1 and NCAD 2 overlays the spectrum of NCAD 12.

Figure 3: Spectral Comparison of Neural Cadherin Domains. (A) UV (B) CD (C) Fluorescence

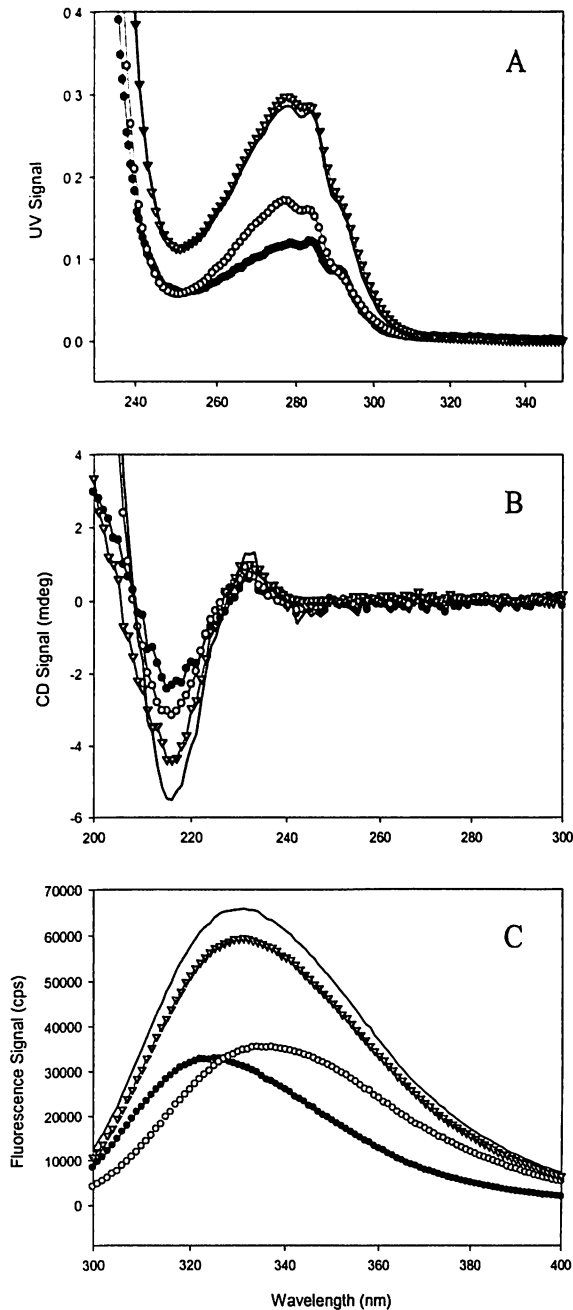


Figure 3: Spectral comparison of Neural Cadherin Domains in the native state. (A) UV spectra comparison of NCAD 1, NCAD 2 and NCAD 12 ($\sim 50 \mu\text{M}$) in SEC Buffer. Spectra were corrected for a buffer blank. (B) CD spectra (mdeg) of $47 \mu\text{M}$ NCAD 1, NCAD 2, and NCAD 12 from 200 to 300 nm (0.2 mm path length). (C) Fluorescence emission spectra of $5 \mu\text{M}$ NCAD 1, NCAD 2 and NCAD 12 with excitation at 280 nm. Note, in each figure the solid line is the sum of the NCAD 1 and NCAD 2 signals.

Extinction coefficient values, calculated based on the signals at 280 nm, are reported in **Table 2**. Values for NCAD 1 are less than that for NCAD 2 consistent with the spectra. The extinction coefficients for Domain 1 constructs were identical. The sum of the extinction coefficients for Domain 1 and 2 is identical to that determined for NCAD 12.

TABLE 2: Extinction Coefficients

Construct	# Trp	# Tyr	Extinction Coefficient
NCAD 1	1	1	7750 ± 440
NCAD 1-L1	1	1	7400 ± 200
NCAD 2	1	4	10800 ± 900
L1-NCAD-L2	1	4	Not Determined
NCAD 12	2	5	19300 ± 800

The CD spectra had a wavelength minimum at approximately 215 nm (**Figure 3B**) which is typical for β -sheet proteins. It is clear that both individual domains are folded. The signal for Domain 1 was less than that of Domain 2. The sum of the spectra from Domains 1 and 2 showed more signal than the NCAD 12 construct.

Fluorescence emission spectra for Domain 1 and Domain 2 were different. Fluorescence emission spectra were blue shifted (320 nm) for Domain 1 and red shifted (336 nm) for Domain 2. The sum of these spectra showed an increase in signal compared to the two-Domain construct but both the sum and the actual NCAD 12 spectra had the same relative maximum at approximately 330 nm.

Temperature Denaturation

Temperature denaturation studies were conducted to determine protein stability. A plot of normalized CD signal of NCAD 1 at 223 nm versus temperature is shown in **Figure 4A**. Transitions were identical with a midpoint of ~ 75 °C. The construct with

the linker and the single Domain 1 both showed identical behavior in the presence and absence of calcium. Data were not fit to Eq. 7 to resolve values of ΔH_m^0 , ΔC_p^0 , and T_m since there was no denatured baseline. Addition of 1 M NaCl had no effect on the profiles (data not shown).

Figure 4B shows similar transitions for NCAD 2 and L1-NCAD-L2. Upon addition of calcium to both constructs there was an increase in temperature ($\sim 9^\circ\text{C}$). It is clear that the linker segments destabilize the domain and calcium stabilizes both Domain 2 constructs. Parameters were resolved to fits to Eq. 7 and are shown in Table 3.

TABLE 3: *T-melt Compilation*

CONSTRUCT	Apo			5 mM Ca^{2+}		
	T_m^a ($^\circ\text{C}$)	$\Delta H_m^0^a$ (kcal/mol)	$\Delta G_{un}^0^b$ (kcal/mol)	T_m^a ($^\circ\text{C}$)	$\Delta H_m^0^a$ (kcal/mol)	$\Delta G_{un}^0^b$ (kcal/mol)
NCAD2	57.6 \pm 1.0	67.3 \pm 3.1	4.97 \pm 0.39	58.7 \pm 0.4	65.5 \pm 1.6	4.88 \pm 0.10
L1-NCAD2-L2	53.7 \pm 0.7	61.4 \pm 3.0	4.10 \pm 0.22	60.2 \pm 0.8	64.6 \pm 2.4	4.90 \pm 0.27

^a Melting temperature (T_m) and enthalpy (ΔH_m) resolved from fits with ΔC_p fixed to 1 kcal/Kmol and R fixed to 0.0019872 kcal/Km.

^b Calculated using Equation 7 at 25 $^\circ\text{C}$.

NCAD 12 shows two transitions in the temperature denaturation. The apo condition has a less well-defined first transition. Addition of calcium shifts the first transition to a significantly higher temperature ($\sim 18^\circ\text{C}$ increase). Interestingly the second transition is unaffected by calcium and has a midpoint of $\sim 75^\circ\text{C}$. Again, the data for NCAD 12 could not be fit due to uncertainty in the unfolded end points.

Reversibility

Reversibility of the unfolding transitions was addressed for NCAD 1, NCAD 2, and NCAD 12 proteins. Solutions of apo-NCAD constructs were unfolded by heating to

90 °C and then refolded by cooling while monitoring CD signal at 230 nm. The refolding transitions for NCAD 2 and NCAD 12 were identical to the melting transitions. NCAD 1 unfolding transition had a sloping baseline that was not observed upon cooling. However, the high temperature transition for NCAD 1 was reversible.

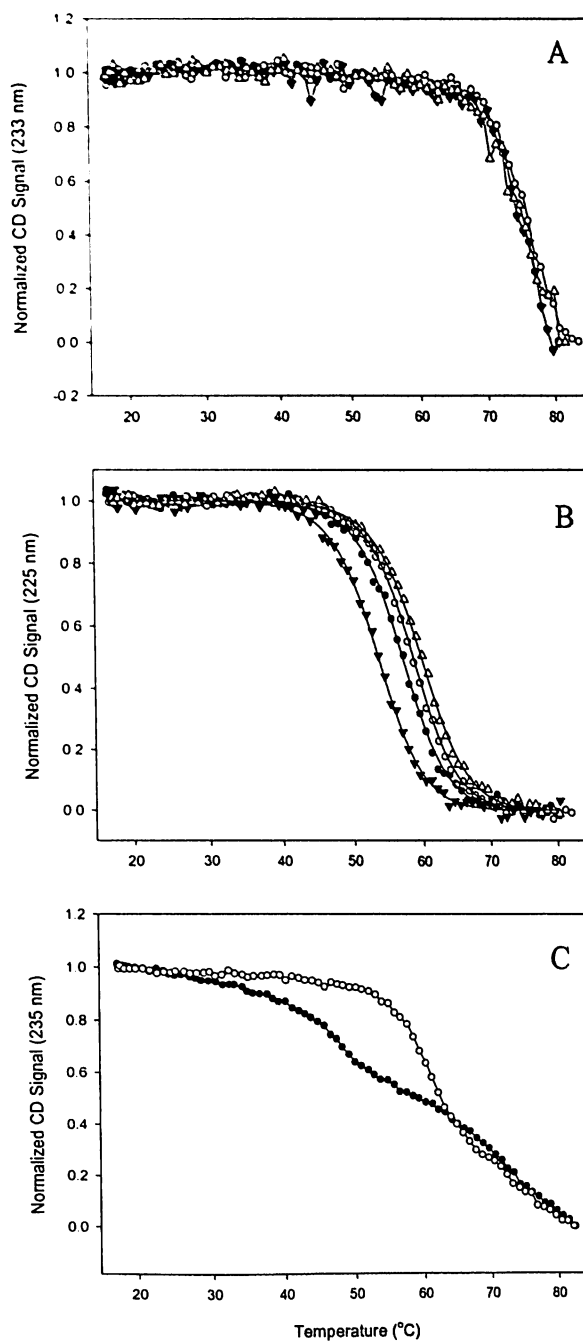


Figure 4: Calcium-dependent temperature induced denaturation of NCAD constructs. (A) Plot of normalized CD signal (mdeg: 233 nm) against temperature (°C) in the presence and absence of calcium. The symbols are data taken of NCAD 1 apo (●) and 5mM calcium (○) and NCAD 1-L1 apo (▼) and 5 mM (▽). (B) Plot of normalized CD signal (mdeg: 225 nm) against temperature in the presence and absence of calcium. The symbols are data taken of NCAD 2 apo (●) and 5mM calcium (○) and L1-NCAD 2-L2 apo (▼) and 5mM calcium (▽) unfolding experiments. (C) Plot of normalized CD signal (mdeg: 230 nm) against temperature for NCAD 12 unfolding experiments in the absence (●) and presence (○) of calcium conditions.

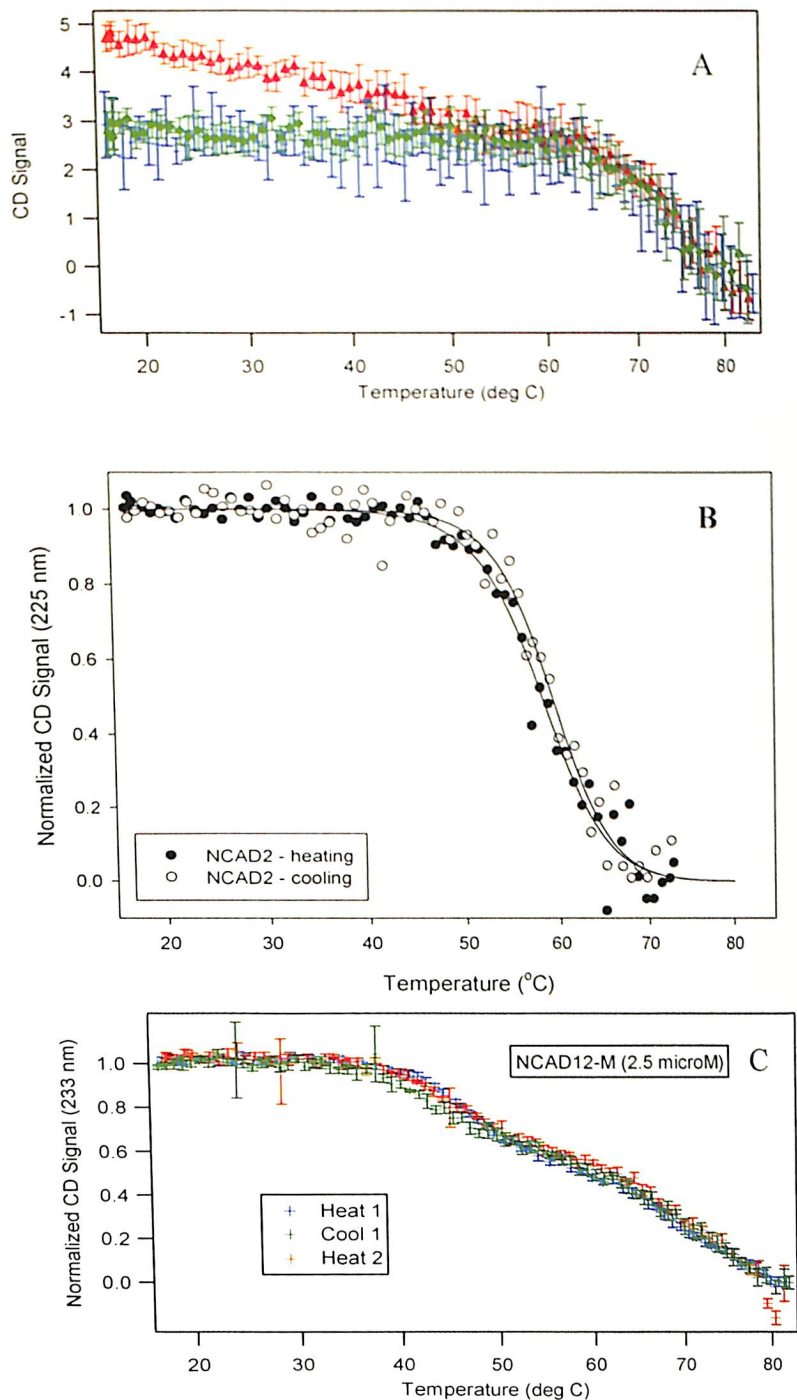


Figure 5: Reversibility of Unfolding Transitions in the apo state: Unfolding and refolding experiments shown in a plot of CD signal versus temperature were conducted on (A) NCAD 1 temperature denaturation in an apo state ($1.94 \mu\text{M}$) from 15 to 90°C (\blacktriangle), from 90 to 15°C (\blacklozenge), and 15 to 90°C ($+$). (B) NCAD 2 temperature denaturation in the apo state from 15 to 90°C (\bullet), 90°C to 15°C (\circ). (C) NCAD 12 temperature denaturation in the apo state from . All experiments were conducted with a 1 cm path length in a quartz cuvette.

DISCUSSION

This study of the first two extracellular domains of neural cadherin encompasses experiments from several undergraduate researchers conducted in the lab of Dr. Susan Pedigo. The major goal is characterization of the first two modular domains of neural cadherin. These studies compare directly to the dissection of ECAD domains as reported in literature (11-13). Despite intense effort on the part of several individuals to purify ECAD 1 or ECAD 1-L1, they were unsuccessful presumably due to instability of the first module of ECAD. ECAD 2 and L1-ECAD 2-L2 were successfully purified and upon characterization of their stability they found that the addition of linker regions significantly destabilized the core domain. We report here characterization of NCAD 1, NCAD 1 and NCAD 12. This study compares the characteristics of NCAD 1 to that of NCAD 2 and asks whether the sum of those characteristics is equal to that of the whole construct, NCAD 12.

Spectral Studies:

UV spectra were typical for a protein that contains tryptophan and tyrosine. Domain 1 showed a decreased absorbance between wavelength 260 and 280 nm which can be attributed to fewer tyrosine residues in comparison to the Domain 2 construct. The sum of the UV spectra for NCAD 1 and NCAD 2 showed a direct correlation with

the spectra for NCAD 12. This indicates that the concentrations of the protein stocks were known and extinction coefficients were well determined.

CD spectroscopy is a technique that yields information about the secondary structure of a protein. CD spectra show characteristic minima at both ~ 222 nm and 208 nm for α -helices and ~ 218 nm for β -sheet. This spectroscopic technique can be utilized in determining the approximate degree of secondary structure as demonstrated in the magnitude of the signal. In this case the CD signal is negative, which means left hand polarized light was absorbed more than right hand polarized light. The more negative the signal values is the greater the signal. The CD studies reported here showed that both single domain constructs were folded in spite of the fact that they were dissected from the context of the whole protein. All spectra showed a minimum at ~ 218 nm, consistent with a β -sheet structure. The sum of the signal of NCAD 1 and NCAD 2 was greater than that of the signal for the NCAD 12 construct. If the increased CD signal is an illustration of an increase in secondary structure, one might infer from these data that NCAD 1 and NCAD 2 interact in the two-domain construct. This interaction is in a way that decreases the secondary structure content. This may be due to electrostatic repulsion between domains in the absence of calcium.

To further evaluate this behavior fluorescence emission spectra were taken to characterize the exposure of the tryptophan. Excitation at 290 nm excites tryptophan residues only and it gives an emission at ~ 330 nm. It is expected that if the tryptophan is in its hydrophobic pocket the spectra will show a blue shift while that of an exposed tryptophan will give a red shift. Data showed a λ_{max} of 320 nm for NCAD 1 and 336 nm for NCAD 2, suggesting that the W2 of NCAD 1 is less exposed in comparison

to the W113 of NCAD 2. This is consistent with the model in which Domain 1 is folded and the W2 is docked into its hydrophobic pocket giving a blue shift in the emission spectra. W113, on the other hand, is partially exposed. We have estimated the exposure of W113 in the NCAD 12 structure by Pertz et al, to be 40% (Surface accessibility by GetArea (14) using the structure 1ff2.pdb (15).

Similar to the CD data, the sum of the fluorescence spectra of NCAD 1 and NCAD 2 exceeds that of NCAD 12. The maximum wavelength of the two is the same illustrating that the W2 and W113 are similarly exposed to buffer when in the individual domains and the two-Domain construct. The difference in the magnitude of the signal illustrates that there is only a small difference in the tryptophan environment in the two-Domain construct. The joining of the two modules in the two-Domain construct causes a small rearrangement in the domains without any large changes in the exposure of the tryptophan residues.

Stability Studies:

Stabilizing effects with and without linker segments in the absence and presence of calcium were also studied. Calcium ions bind at the interface between extracellular domains causing the adhesive dimer formation. Previous experiments with ECAD have given rise to the theory that alterations in the whole domain construct will affect the folding of the domain. Based on the experiments of the dissection of ECAD domains we expected the following: 1) Domain 1 to be less stable in isolation than in the two-domain construct, 2) Domain 2 to be more stable than Domain 1, 3) Addition of linkers to destabilize Domain 2, but perhaps stabilize Domain 1, 4) Individual domain constructs should not bind calcium with the same affinity as NCAD 12, since the individual

domains do not have a complete calcium binding pocket, 5) All constructs should be stabilized by addition of calcium or NaCl. Considering these predictions, only NCAD2 constructs behaved predictably.

The unfolding of NCAD 2 is characterized by its melting at ~ 57.6 °C. Data shows that NCAD 2 was significantly destabilized upon addition of linkers such that L1-NCAD 2-L2 melted at 53.7 °C. This is less difference than was observed for the identical ECAD 2 constructs (differed by 9 °C). We attribute this decrease in melting temperature to the electrostatic repulsion between clusters of negatively charged residues within the loops that connect the beta sheets and the aspartates in the linker segments. Addition of calcium stabilized both NCAD 2 constructs. The construct with the linkers was stabilized more since the linker provides a more complete binding pocket for calcium. Thus, NCAD 2 behaved predictably.

Studies of Domain 1 present the largest differences between ECAD and NCAD. ECAD 1 was not stable enough to purify. Upon separation from Domain 2, the Domain 1 construct could not be isolated. We believed the same might be true for NCAD 1. However, we were able to purify NCAD 1, implying that ECAD 1 and NCAD 1 do not have the same stability and that NCAD 1 is more stable than ECAD 1. Melting profiles of NCAD 1 showed a melting transition well above average temperature for a small, 100 residue, globular protein (see table in (11)). We propose a model later in the discussion.

The NCAD 12 denaturation profile shows two melting transitions. The first transition occurs at ~ 50 °C. This first transition appears to match what we might expect for Domain 2. The second transition occurs at ~ 74 °C, a similar transition as observed for Domain 1. Thus, the melting of the two-Domain construct appears to be the simple

sum of the melting of Domain 1 (first transition) and Domain 2 (second transition). What is a reasonable expectation for the melting temperature for Domain 1?

We expect that Domain 1 should melt between ~37 and 45 °C for two reasons. First, as discussed briefly in the Materials and Methods section, we can separate the stable noncovalent dimer that forms in our stocks by simply heating the solutions to 37 °C. This implies that Domain 1 releases the strand β A crossover structure at this temperature, and that Domain 1 might unfold. Secondly, we do not expect it to be more stable than Domain 2, based on the similarity between the primary, secondary and tertiary structures of ECAD 12 and NCAD 12. As is true for ECAD 12, we expect that Domain 1 will unfold at temperatures no higher than needed to unfold Domain 2 (~ 50 °C).

The proposed model by which the high temperature transition occurs is assumed to be as follows: W2 is released from its docked position in the hydrophobic pocket at ~37 °C, NCAD 1 unfolds no later than ~50 °C, NCAD 2 unfolds at ~50 °C, at ~60 °C the atypical secondary structure formation occurs and at ~74 °C the atypical secondary structure melts. The formation of the atypical secondary structure requires Domain 1.

Studies of Reversibility of Unfolding Transitions

Reversibility of the unfolding transitions was illustrated by heating, cooling and reheating the protein samples. Transitions were remarkably reversible with one exception. Data of Domain 1 were not normalized and were left as raw data because it had an obvious sloping baseline. This “first transition” or sloping baseline is not reversible. Surprisingly, the second transition is reversible. What is this atypical secondary structure? We considered an aggregate formation or plaque like structure but ruled it out due to experimental data showing that there is no dependence on protein

CONCLUSION

Careful analysis of data collected from CD, UV-vis, fluorescence spectra and thermal-stability studies over a several year period have given insight into the characteristics and thermal stability of the extracellular domains of neural cadherin. This study provides important observations of structure and stability. First, the unique characteristics of NCAD 1 show that it is distinctively different from ECAD 1. It can be purified, whereas ECAD could not. We found that linker segments destabilized NCAD 2 domain constructs while any effect of linkers on NCAD 1 was masked due to the high temperature melting transition. The melting temperature was expected to be much lower than the obtained 74 °C. We hypothesize that the protein melted and then the atypical structure formed. NCAD 12 construct showed significant stabilization upon addition of calcium. The sum of the individual domains leads to minor changes when in the two-domain construct, signifying changes in the tryptophan environment but not the degree of exposure to solvent. The conclusion of an atypical secondary structure at high temperature deserves further experimentation to confirm what is actually occurring.

REFERENCES

1. Nollet, F., Kools, P., and van Roy, F., Phylogenetic analysis of the cadherin superfamily allows identification of six major subfamilies besides several solitary members, *J Mol Biol*, 299, 551 (2000).
2. Chothia, C., and Jones, E. Y., The molecular structure of cell adhesion molecules, *Annu Rev Biochem*, 66, 823 (1997).
3. Troyanovsky, R. B., Sokolov, E., and Troyanovsky, S. M., Adhesive and lateral E-cadherin dimers are mediated by the same interface, *Mol Cell Biol*, 23, 7965 (2003).
4. Gumbiner, B. M., Cell adhesion: the molecular basis of tissue architecture and morphogenesis, *Cell*, 84, 345 (1996).
5. Adams, C. L., and Nelson, W. J., Cytomechanics of cadherin-mediated cell-cell adhesion, *Curr Opin Cell Biol*, 10, 572 (1998).
6. Kemler, R., From cadherins to catenins: cytoplasmic protein interactions and regulation of cell adhesion, *Trends Genet*, 9, 317 (1993).
7. Harrison, O. J., Corps, E. M., Berge, T., and Kilshaw, P. J., The mechanism of cell adhesion by classical cadherins: the role of domain 1, *J Cell Sci*, 118, 711 (2005).
8. Nagar, B., Overduin, M., Ikura, M., and Rini, J. M., Structural basis of calcium-induced E-cadherin rigidity and dimerization, *Nature*, 380, 360 (1996).
9. Shapiro, L., Fannon, A. M., Kwong, P. D., Thompson, A., Lehmann, M. S., Grubel, G., Legrand, J. F., Als-Nielsen, J., Colman, D. R., and Hendrickson, W. A., Structural basis of cell-cell adhesion by cadherins [see comments], *Nature*, 374, 327 (1995).

10. Salinas, P. C., and Price, S. R., Cadherins and catenins in synapse development, *Curr Opin Neurobiol*, *15*, 73 (2005).
11. Prasad, A., Housley, N. A., and Pedigo, S., Thermodynamic stability of domain 2 of epithelial cadherin, *Biochemistry*, *43*, 8055 (2004).
12. Prasad, A., Zhao, H., Rutherford, J. M., Housley, N. A., Nichols, C., and Pedigo, S., Effect of linker segments upon the stability of Epithelial-Cadherin Domain 2, *Proteins*, *62*, 111 (2006).
13. Prasad, A., and Pedigo, S., Calcium-dependent Stability Studies of Domains 1 and 2 of Epithelial Cadherin, *Biochemistry*, *44*, 13692 (2005).
14. Frackiewicz, R., and Braun, W., Exact and efficient calculation of the accessible surface areas and their gradients for macromolecules, *J. Comp. Chem.*, *19*, 319 (1998).
15. Pertz, O., Bozic, D., Koch, A. W., Fauser, C., Brancaccio, A., and Engel, J., A new crystal structure, Ca²⁺ dependence and mutational analysis reveal molecular details of E-cadherin homoassociation, *Embo J*, *18*, 1738 (1999).